https://doi.org/10.48047/AFJBS.6.11.2024. 125-145

African Journal of Biological Sciences

Chest X-Ray Image Classification: DenseNet169 Model for Medical Diagnostics

[1]Munesh Meena, [2]Ruchi Sehrawat

*[1, *] Research Scholar, University School of Information Communication & Technology, GGSIPU, Delhi, India.*

[2]Assistant Professor, University School of Information Communication & Technology, GGSIPU, Delhi, India.

**Corresponding author: munesh8204@gmail.com*

Article History
Volume 6, Issue 11, 2024
Received: 02 Jun 2024
Accepted: 15 Jun 2024
doi: ***10.48047/AFJBS.6.11.2024.125-145***

Abstract: The global health crisis caused by COVID-19 has highlighted the need for accurate diagnostic methods. Traditional testing methods face challenges due to their cost, the invasive nature of the tests, and potential errors. This research paper proposes densely convolutional neural network models for the classification of chest X-ray images, focusing on distinguishing between COVID-19, Normal, and Pneumonia cases. The study also compares the performance of different proposed Convolution Neural Network (CNN) architectures: DenseNet121, DenseNet169, and DenseNet201 with earlier reported work. Our analysis revealed that the proposed DenseNet169 outperformed the other models related to previous studies across key performance metrics. It achieved an impressive accuracy of 96% and the highest precision at 97%, while the proposed DenseNet121 and DenseNet201 also displayed high accuracy and low loss values, they did not match the overall balance of precision, recall, and F1-score provided by DenseNet169.

Keywords: COVID-19 Diagnosis, Deep Learning, DenseNet, Chest X-ray Imaging, Convolutional Neural Networks, Transfer Learning

1. **Introduction:** Improving global living standards heavily relies on healthcare research, which aims to enhance diagnostic accuracy, benefiting both medical professionals and patients by minimizing the chances of misdiagnosis and unnecessary treatments [1]. One of the key advancements in this field is the use of computer systems equipped with advanced image processing technologies, which are known for their speed and precision in generating results [2]. Deep learning, especially Convolutional Neural Networks (CNN), has gained prominence

in processing medical images, including radiographs, significantly contributing to automated disease detection [3, 4].The COVID-19 pandemic, which emerged in Wuhan, China in late 2019, rapidly escalated into a global crisis. It led to millions of infections and fatalities worldwide, showcasing a broad spectrum of symptoms [5, 6, 7]. The virus's ability to mutate has resulted in various strains, each differing in transmission rates and symptomatology [8]. The conventional COVID-19 detection methods, such as RT-PCR, are criticized for being invasive and time-consuming, with varying accuracy, prompting the exploration of alternatives like chest X-rays for diagnosis [10]. The application of computer-generated imaging in detecting lung infections offers advantages like quick triaging and accessibility, although it requires confirmation through PCR tests for complete accuracy [11, 12]. Pneumonia, which often presents symptoms similar to COVID-19, is a significant lung infection that ranges from mild to severe and is particularly deadly for young children. It's classified based on different factors, including its origin and causative pathogens [13, 14, 15, 16, 17]. The integration of AI, especially deep learning and machine learning, has enhanced the diagnosis of both COVID-19 and pneumonia through the analysis of chest X-rays. These technologies excel in pattern recognition, vital for differentiating between various lung infections [9, 15]. CNNs are especially useful in medical diagnostics due to their ability to extract complex patterns from images, videos, or audio without the need for preprocessing [16, 18, 19, 20]. Various CNN architectures, such as VGG, ResNet, Xception, and DenseNet, have been adapted to detect COVID-19 and pneumonia in lung X-rays with high accuracy [21].Illnesses resembling pneumonia, especially during flu seasons, tend to be more contagious [22], [23]. Chest X-rays are essential in healthcare, aiding radiologists in identifying pneumonia types and causes [24]. X-rays are commonly used to screen and diagnose various chest diseases, including pneumonia, tuberculosis, and breast cancer, owing to their non-invasive nature, suitability for large-scale use, and cost-effectiveness [25].The COVID-19 pandemic has presented enormous challenges to governments and healthcare systems across the globe [26], [27], [28]. It was declared a Public Health Emergency of International Concern in January 2020 and was officially named COVID-19 by the World Health Organization (WHO) in February 2020. By March 2020, it was recognized as a global pandemic [29], [30]. The symptoms of COVID-19 are predominantly respiratory, but some patients also experience gastrointestinal issues [31], [32]. Various detection methods, including RT–PCR, LAMP, and antigen testing, are used for identifying COVID-19. While RT–PCR is highly specific, its sensitivity in detecting the virus has been relatively low [32], [27].

2. **Related Work:** Historically, research has heavily focused on pneumonia because of its significant impact on health. This emphasis continued even with the emergence of the coronavirus pandemic, with studies investigating pneumonia's origins for more effective treatments. Concurrently, there's been an exploration into the use of machine learning for the quick, non-invasive identification and differentiation of COVID-19 cases. Khan et al. [19] developed a model known as STM-RENet, based on the split-transform-merge concept, to recognize COVID-19 in chest X-ray images. They tested this model on three different datasets,

including an augmented one, and evaluated how channel boosting improved the model's performance, finding that the channel-boosted version (CB-STM-RENet) was superior in accuracy and other metrics. Another study by Khan et al. [21] focused on distinguishing COVID-19 from viral pneumonia using various deep learning models. They used a large collection of chest X-ray images and applied pretrained feature extractors like NasNetMobile, EfficientNetB1, and MobileNetV2. EfficientNetB1, particularly with batch normalization, proved to be the most accurate after fine-tuning and applying different training approaches. Chakraborty et al. [33] also pursued differentiating COVID-19 from pneumonia using deep learning. Their dataset, sourced from Kaggle and GitHub, was preprocessed and segmented with the FC-DenseNet103 algorithm, and using the ResNet18 architecture, they achieved high accuracy and sensitivity. Xu et al. [34] created a model named "MANet" to differentiate COVID-19 from normal cases, tuberculosis, and pneumonia. They combined three public datasets and used a two-stage approach involving segmentation and classification. Their findings indicated that incorporating Mask Attention (MA) technology enhanced the performance of classifiers, with ResNet50 being the most accurate. Thakur et al. [35] worked on both binary and multiclass classification of COVID-19 using two CNN models to analyze chest X-rays and CT scans. Utilizing two datasets for binary and multiclass classification, they achieved notable accuracy and F1-scores in both. Artificial intelligence has made a significant impact in medical imaging and other medical fields [36]. Radiological imaging, like chest X-ray scans, plays a vital role in effectively managing patient care, isolating infected individuals, and precisely identifying different types of pneumonia. A. Narin et al. [37] employed five CNN models (ResNet50, ResNet101, ResNet152, InceptionV3, and Inception-ResNetV2) to detect coronavirus pneumonia through chest X-rays. M. Turkoglu [38] used AlexNet's convolutional and fully connected layers, enhanced through transfer learning, and combined them with a Relief-identified SVM classifier for identifying key features. This was further improved by integrating the VGG16 pretrained model with data augmentation and patching techniques (RICAP) to differentiate between healthy individuals and COVID-19 cases [39]. Khan et al. [40] introduced CoroNet, a deep convolutional neural network model, for automatically detecting diseases from chest X-rays. This model effectively categorized images into three classes: COVID-19, pneumonia, and healthy, with 95% classification accuracy. Ouchicha et al. [41] developed CVDNet, another deep convolutional neural network model using chest X-ray images to classify COVID-19 infections and differentiate them from normal and other pneumonia cases. CVDNet's architecture is based on a residual neural network and features two parallel layers with varying convolution kernel sizes to capture both local and global image features.While these methods have shown encouraging results, especially in binary classification scenarios, they face challenges in maintaining accuracy in three-category classifications (healthy, common pneumonia, and COVID-19). This highlights an ongoing challenge in achieving precise classification across multiple categories, underscoring the advancements in machine learning for the effective and rapid detection of respiratory infections, including COVID-19.

3. Materials and Methods:

3.1. Dataset

In this research, we prioritized achieving high accuracy and precision in detection. To support this goal, we selected a substantial dataset, specifically the "Chest X-ray (Covid-19 & Pneumonia)" dataset from Kaggle. This dataset comprises a total of over 6432 chest X-ray images, which are divided into three distinct categories: COVID-19 positive, Normal, and Pneumonia positive. To facilitate effective model training and evaluation, we divided the dataset into two parts: a training set consisting of 5144 images and a testing set comprising 1288 images. The testing set represents 20% of the entire dataset. This division was crucial for ensuring the reliability and validity of our study's findings. The specific situation of the chest X-ray dataset prepared by us is presented in Table 1.

Table 1 Distribution of different types of data in the dataset.

Data	Training Dataset (80%)	Testing Dataset (20%)	Total Dataset (100%)
COVID-19	460	116	576
NORMAL	1266	317	1583
PNEUMONIA	3418	855	4273
Total	5144	1288	6432

3.2. Image Preprocessing

The Image datasets were preprocessed for optimal model training. The steps are as follows:

- **Image Resizing and Normalization**: We resized all images to a consistent size of 224x224 pixels, matching the dimensions used for ImageNet data, which the network was initially trained on. This uniformity is important for compatibility with the network architecture. Following resizing, each image was normalized. Normalization adjusts the distribution of the input data to be more consistent with the data the pre-trained model was initially trained on.
- **Image Augmentation**: We employed various image augmentation techniques, such as random rotations, shifts, and flips. These methods significantly increase the diversity of features within the training dataset, helping the model learn from a wider range of scenarios. This process not only reduces the likelihood of overfitting but also enhances the model's ability to generalize to new unseen data.
- **Batch Processing**: Images were processed in batches, each containing 32 images. Batch processing is a crucial strategy for managing memory efficiently, especially when dealing with large datasets. It eliminates the need to load the entire dataset into memory at once.

- **Label Encoding and Shuffling**: For the multi-class classification task, we employed one-hot encoding for the labels. Additionally, the images in the training dataset were shuffled at the beginning of each epoch. This shuffling is essential to prevent the model from developing biases towards any particular sequence in which the data is presented.
- **Directory-Based Data Organization**: The images were organized and loaded based on their directory structure. Each subdirectory was named according to its respective class label, facilitating an organized and efficient way to link images with their labels. This organization greatly simplifies dataset preparation. Fig.1 illustrates an example of the acquired images in our dataset.

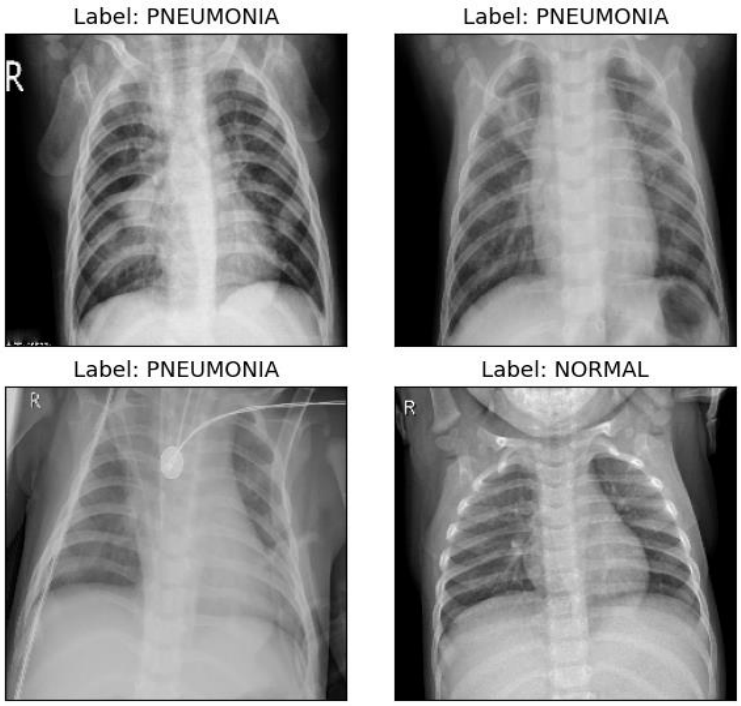

Fig.1. Example of the images acquired from the dataset.

4. Proposed Work:

4.1 Densenet121: In this work, we have developed image classification model based on the DenseNet121 architecture renowned for its efficiency in feature extraction and reduced computational burden due to its dense connectivity pattern. Leveraging the transfer learning model, the model initiates with pre-trained weights from the ImageNet dataset, providing a robust foundational base. We further refine this model for our specific task by incorporating a Global Average Pooling (GAP) layer and a custom fully connected classification layer, the latter being tailored to our dataset's number of classes and employing a softmax activation function for multi-class categorization. This approach strategically balances the benefits of pre-existing deep learning knowledge with the adaptability to new, task-specific requirements.

Training is conducted using categorical crossentropy as the loss function and the Adam optimizer, with an initial phase where the DenseNet121 layers are frozen to consolidate the learned features. This model is constructed with a series of convolutional, batch normalization, and pooling layers, culminating in a total of 7,040,579 parameters, of which only 3,075 are trainable due to the application of transfer learning. The DenseNet121 backbone is augmented with a Global Average Pooling (GAP) layer, reducing the spatial dimensions to a single 1024-dimensional vector per image. This vector is then fed into a dense layer with three output nodes corresponding to the three classes in our study. The model's strength lies in its ability to leverage pre-trained weights from ImageNet, significantly reducing the need for extensive training data, and ensuring efficient feature extraction. This setup is particularly advantageous for tasks requiring high-level feature recognition from limited datasets, as it combines the robustness of DenseNet121's deep architecture with the specificity of a fine-tuned classification layer.

4.1.1 Proposed Algorithm for DenseNet121 Training Model

Input: *Image dataset D. Pre-trained DenseNet121 model weights from ImageNet. Number of classes C.*

Initialize: *Load DenseNet121 architecture with pre-trained ImageNet weights. Freeze DenseNet121 layers.*

Add Custom Layers: *Append a Global Average Pooling (GAP) layer and a Dense layer with C units and softmax activation to the model.*

Compile: *Compile the model using Adam optimizer and categorical crossentropy loss function.*

Pre-process: *Normalize and preprocess images from dataset D to match ImageNet standards.*

Data Augmentation: *Perform image augmentation on D to generate a more diverse training set.*

Train-Test Split: *Split D into training set Dtrain and validation set Dval.*

Training *Phase:* *Train the model on Dtrain with DenseNet121 layers frozen.*

Unfreeze and Fine-Tune (Optional): Unfreeze some/all of the DenseNet121 layers and continue training for fine-tuning.

Training Loop:

- *for each epoch:*
  - *for each batch in Dtrain:*
    - *Perform a forward pass, compute the loss, and backpropagate the errors.*
    - *Update the model parameters of the custom layers (and optionally unfrozen DenseNet121 layers).*
  - *Validate the model on Dval to monitor performance and apply model checkpointing based on validation accuracy.*

Output: *A refined DenseNet121 model tailored for C-class image classification.*

4.2 Densenet169: The core concept of DenseNet169 is its unique connectivity pattern, where each layer is directly connected to every other layer in a feed-forward fashion. This approach ensures maximum information flow between layers in the network. Our DenseNet169 model

is structured into five dense blocks, each comprising multiple layers of batch normalization (BatchNorm), activation functions (ReLU), and convolutional operations (Conv2D). These blocks are interspersed with transition layers that adjust the feature-map size using convolution and pooling operations. The key advantage of this architecture is its ability to reuse features through the network, enhancing feature propagation and reducing the number of required parameters. The first dense block starts with an initial convolutional layer with a 7x7 kernel, followed by a series of convolutional layers with smaller 3x3 kernels. Each convolutional layer within a block adds its output to the inputs of all subsequent layers, growing the feature-map size. Transition layers, consisting of convolution and pooling, are used to reduce the dimensionality of the feature maps between the dense blocks, preventing the model from becoming too computationally intensive. The final dense block in our model outputs a feature map of dimensions 7x7x1664. This output is then processed through a global average pooling layer, which condenses the feature map into a single 1664-dimensional vector. This vector captures the essence of the input image in a form that can be used for classification. Finally, a dense layer with three output nodes is used, corresponding to the number of classes in our study. This layer acts as the classifier on top of the feature extractor formed by the DenseNet169 architecture. The total number of parameters in this model is approximately 12.65 million, of which a mere 4,995 are trainable.

4.2.1 Proposed Algorithm for DenseNet169 Training Model

Input: *Image dataset D. Number of classes C. Pre-trained DenseNet169 architecture.*
Initialize: *Load DenseNet169 with pre-trained weights. Configure each of the five dense blocks with BatchNorm, ReLU, and Conv2D.*
Construct Dense Blocks:

- *Start with an initial Conv2D layer with a 7x7 kernel.*
- *Add subsequent Conv2D layers with 3x3 kernels in each dense block, ensuring direct connectivity from each layer to all subsequent layers.*
- *Introduce transition layers between dense blocks comprising convolution and pooling to reduce feature-map dimensions.*

Compile: *Compile the model using a Adam optimizer and categorical cross entropy loss function.*
Pre-process: *Adapt the input dataset D for the DenseNet169 input requirements(image resizing, normalization).*
Data Augmentation: *Apply augmentation techniques to D to prevent overfitting and improve model robustness.*
Train-Test Split: *Divide D into training set Dtrain and validation set Dval.*
Training:

- *for each epoch:*
  - *for each batch in Dtrain:*
    - *Conduct a forward pass through the dense blocks and transition layers.*
    - *Apply global average pooling to the output of the last dense block.*
    - *Pass the result through a final dense classification layer with C output nodes.*
    - *Compute loss and gradients, then update trainable parameters.*
  - *Evaluate on Dval to assess model accuracy and performance.*

Output: *A trained DenseNet169 model for C-class image classification with a feature-map output of 7x7x1664.*

4.3 Densenet201: In this research, we employed DenseNet201 model, specifically designed to address high-level image recognition tasks. Our model consists of 18327747 parameters, of which only 5763 are trainable, highlighting the model's efficiency by leveraging a high degree of parameter sharing. The architecture is composed of densely connected blocks where each layer is directly connected to every other layer in a feed-forward fashion within a block. This facilitates the model in learning an ensemble set of features at varying levels of abstraction. The model culminates in a global average pooling layer that reduces the spatial dimensions to a singular vector of 1920 features. These features are then fed into a fully connected dense layer with 3 units, corresponding to the number of classes for our classification task. This dense layer is the only part of the model with trainable parameters, ensuring a lightweight fine-tuning process on top of the pre-trained DenseNet features. The employment of batch normalization and relu activation functions are crucial in stabilizing

the learning process and introducing non-linearity, contributing to the model's ability to capture complex patterns within the data. The presented CNN showcases a blend of depth and efficiency, making it a robust choice for image classification within the constraints of our computational resources.

4.3.1 Proposed Algorithm for DenseNet201 Training Model

Input: *Image dataset D. Pre-trained DenseNet201 model. Number of classes C.*
Initialize: *Load DenseNet201 architecture with pre-trained weights. Configure densely connected blocks for feature extraction.*
Set Trainable Parameters: *Mark only the final dense layer's parameters as trainable, total of 5,763.*
Compile: *Compile the model with an Adam optimizer and categorical crossentropy loss function.*
Pre-process: *Prepare dataset D according to DenseNet201 input requirements (image resizing, normalization).*
Data Augmentation: *Implement data augmentation on D to generate a diverse training set and prevent overfitting.*
Train-Test Split: *Partition D into training set Dtrain and validation set Dval.*

Training Process:

- for each epoch:
  - for each batch in *Dtrain*:
    - *Execute a forward pass through the dense blocks.*
    - *Apply global average pooling to obtain a 1920-feature vector.*
    - *Input the vector into the final dense classification layer with C units.*
    - *Calculate loss, perform backpropagation, and update the 5,763 trainable parameters.*
  - *Evaluate model accuracy and performance on Dval.*

Output: *A DenseNet201 model fine-tuned for a C-class image classification task*

5 Results and Analysis:

5.1 Densenet121: In our study, we evaluated the performance of a deep learning model designed to differentiate between COVID-19, normal, and pneumonia conditions using chest X-ray images. The confusion matrix in fig.4 provides a visual depiction of the performance of our classification model. The matrix elucidates the number of correct and incorrect predictions made by the model with respect to the true labels.

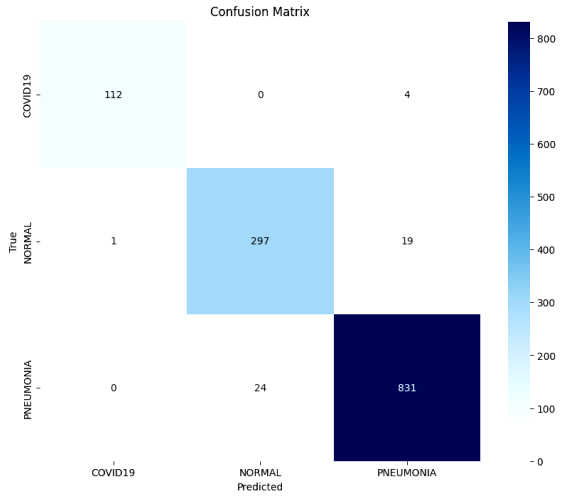

Fig.4. Confusion Matrix of DenseNet121 Classification Model

For COVID-19, the model correctly identified 112 out of 116 cases, with 4 cases misclassified as Pneumonia, showcasing a high true positive rate. In the case of normal chest X-rays, out of 317 instances, 297 were accurately classified while 19 were incorrectly identified as Pneumonia and 1 as COVID-19, indicating a relatively small confusion with other conditions. For Pneumonia predictions, the model impressively recognized 831 out of 855 cases, with a small number of 24 cases being misinterpreted as normal.

In fig. 5(a) and 5(b), we observe the model's accuracy and loss metrics over successive epochs during training and validation phases. The left graph showcases the accuracy trends, where the training accuracy (blue line) indicates the proportion of correct predictions made by the model on the training dataset, and the validation accuracy (orange line) reflects the model's performance on a separate, unseen dataset. After an initial sharp increase, both accuracies level off, with the validation accuracy slightly undulating but remaining close to the training accuracy, suggesting that the model generalizes well without overfitting.

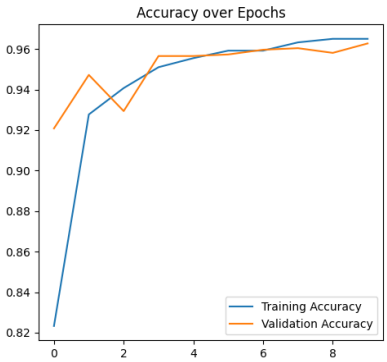

Fig.5 (a) Accuracy over Epochs

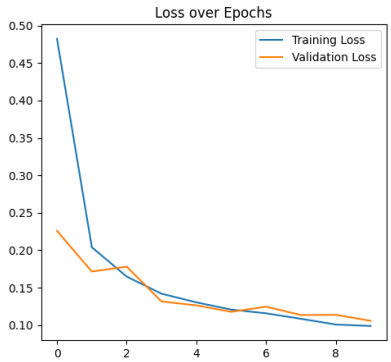

Fig.5 (b) Loss over Epochs

The right graph illustrates the model's loss, a measure of the prediction error, over the same epochs. The training loss (blue line) decreases significantly over the first few epochs, indicating that the model is learning to fit the training data effectively. The validation loss (orange line) also decreases but shows a convergence with the training loss, which is indicative of a well-fitting model.

5.2 Densenet169: In the evaluation of the DenseNet169-based convolutional neural network model for classifying medical images into three categories—COVID-19, Normal, and Pneumonia—the model achieved high performance across all metrics. The confusion matrix in fig.6 provides a visual representation and assessment of the model's performance across the three classes: COVID-19, Normal, and Pneumonia. For COVID-19, out of 116 actual cases, the model correctly identified 112, with only 2 false negatives and 2 false positives, indicating a high true positive rate and specificity.

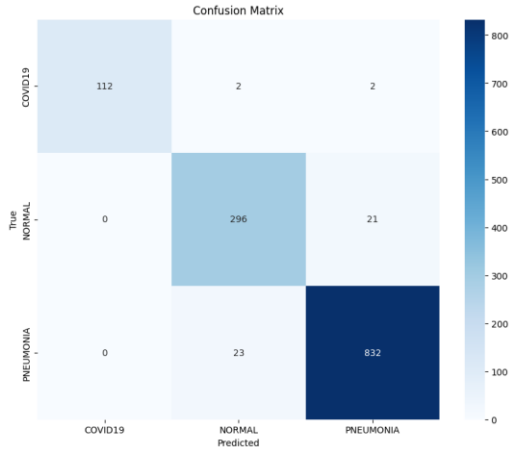

Fig.6. Confusion Matrix of DenseNet169 Classification Model

The Normal category showed no false negatives, with 296 true positives and 21 false positives, suggesting that while the model is highly accurate in identifying Normal cases, there is some confusion with the Pneumonia class. For the Pneumonia class, the model demonstrated a strong predictive power with 832 true positives out of 855 actual cases, and only 23 false negatives, indicating a very high sensitivity and ability to correctly identify the majority of pneumonia instances. The graphical representation of the model's learning process over the course of training epochs is depicted in two plots: Fig.7 (a) Accuracy over Epochs and Fig.7 (b) Loss over Epochs. The Accuracy over Epochs graph shows a convergence pattern between the training and validation accuracy, indicative of a well-fitting model. Initially, the training accuracy starts at around 88% and experiences a steep increase, stabilizing near 96% by the end of the training process. Conversely, the Loss over Epochs graph demonstrates a decreasing trend, where both training and validation loss diminish significantly over time, which is a characteristic of effective learning

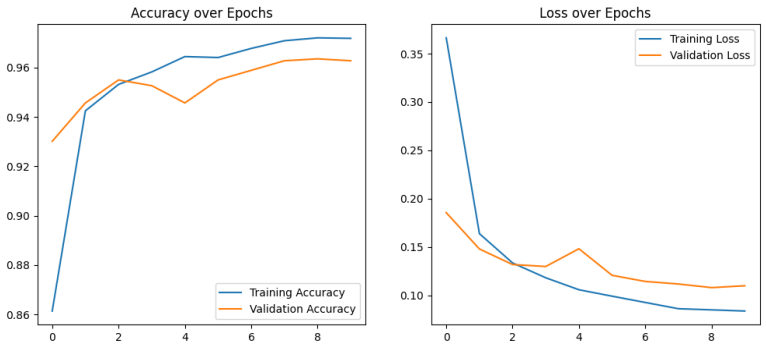

Fig.7 (a) Accuracy over Epochs **Fig.7 (b) Loss over Epochs**

5.3 Densenet201: In the evaluation of the classification model, which was designed to discern between COVID-19, normal, and pneumonia cases from chest X-ray images, the model's performance was evaluated using the confusion matrix of the classification model in fig.8 provides a detailed breakdown of its performance across the three classes: COVID-19, Normal, and Pneumonia. Each entry in the matrix represents the number of instances that were predicted in each classification compared to the true labels.

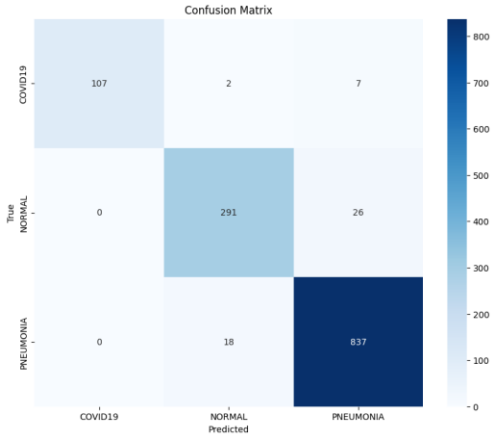

Fig.8. Confusion Matrix of DenseNet201 Classification Model

For the COVID-19 class, out of 116 true cases, the model accurately identified 107, incorrectly predicting 2 as Normal and 7 as Pneumonia, demonstrating high sensitivity towards the COVID-19 class with few misclassifications. In the case of Normal X-rays, the model correctly predicted 291 out of 317 instances, with 26 being misclassified as Pneumonia, indicating a robust ability to distinguish normal cases, albeit with a slightly higher confusion with Pneumonia. The model showed a strong performance in identifying Pneumonia, correctly classifying 837 out of 855 instances, with only 18 being incorrectly labeled as Normal. The training process of the deep learning model over successive epochs is depicted in two graphs, illustrating the accuracy and loss metrics for both the training and validation datasets. The 'Accuracy over Epochs' fig.8 (a) displays a positive trend, with the training accuracy starting at around 91% and showing a sharp increase, stabilizing at

approximately 97%. Conversely, the 'Loss over Epochs' fig.8 (b) exhibits an inverse relationship, where both training and validation loss decrease rapidly initially, with the training loss stabilizing at a low level.

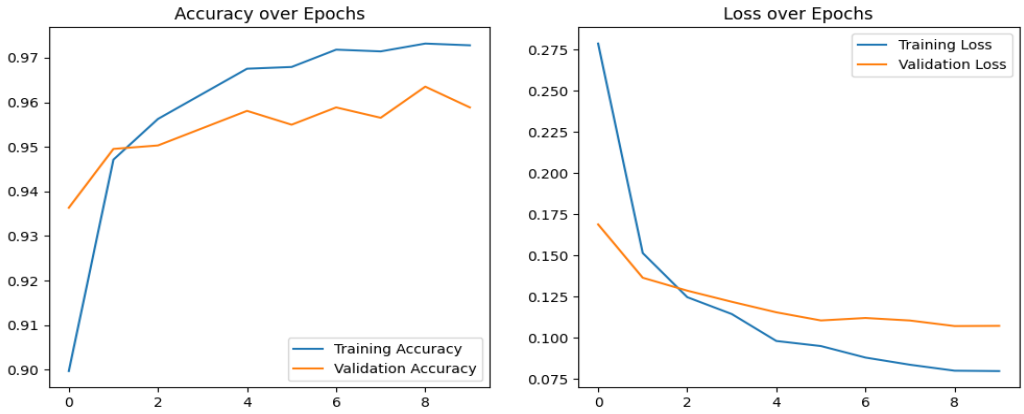

Fig.8 (a) Accuracy over Epochs **Fig.8 (b) Loss over Epochs**

Overall, the performance metrics captured in these graphs signify a robust learning process, with the model achieving high accuracy and low loss, a strong indication of its ability to generalize well when presented with new data. However, the slight divergence of validation loss calls for a careful observation to ensure that the model does not start overfitting as it continues to learn.

Performance Comparison: Table 5 presenting the performance of the Sequential CNN, DenseNet121, DenseNet169, and DenseNet201 models.

Table 2 Performance comparison of the models

Model	Accuracy	Precision (Macro Avg.)	Recall (Macro Avg.)	F1-Score (Macro Avg.)	Loss	Strengths	Limitations
DenseNet121	96%	96%	96%	96%	Low	High precision and recall	Moderately complex
DenseNet169	96%	97%	96%	96%	Very Low	Highest precision among models	Higher complexity

DenseNet201	96%	97%	94%	95%	Low	High precision, robust learning	Highest complexity and computational needs

Table 3 presenting the performance comparison with earlier reported work

Table 3 Comparative Performance of CXR Image Analysis Models for Pneumonia, COVID-19 Detection

Authors	Dataset	Model	Performance (%)
Varshini et al. (2019)	Kaggle	DenseNet-169+ SVM	AUC = 80.2%
Rahman et al. (2020)	Kaggle	AlexNet SqueezeNet ResNet18 DenseNet201	Accuracy = 99% Precision = 96% Recall = 93.2%
Zhang et al. (2021)	Kaggle	VGG-based CNN model	Accuracy = 96.4% Precision = 96.7% Recall = 93.2% F1 score = 94.8%
Manickam et al. (2021)	Kaggle	ResNet50	Accuracy = 93.06% Precision = 88.97% Recall = 92.76% F1 Score = 90.68%
Zhang et al. (2021)	Kaggle	VGG-based model architecture with fewer layers	Accuracy = 94.068% Precision = 96.00% Recall = 90.83% F1 score = 92.851%
Kundu et al. (2021)	Kermy RSNA	Ensemble of three CNN models: GoogLeNet, ResNet-18 and DenseNet-121	Sensitivity = 86.85% Sensitivity = 87.02% Precision = 86.89%
Lin et al. (2022)	RSNA	SAS-MFF-YOLO	Precision = 88.1% Recall = 82.8%
Wang et al. (2020)	COVIDx	U-Net+ Ensemble COVID-Net	Accuracy = 93.3% Sensitivity = 91.0%
Singh et al. (2021)	Public dataset	Multi-objective adaptive differential evolution based CNN	Accuracy = 94.48% Sensitivity = 93.3% Specificity = 94.58% F-measure = 93.89%
Mahajan et al. (2022)	COVIDx Mendeley	Ensemble of DenseNet201+ Single Shot MultiBox Detector (SSD)	Precision = 93.01% Recall = 94.98% F1-score = 93.98%
Arifin et al. (2021)	Public	Single Shot Detection MobileNet Y1 Single Shot Detection MobileNet Y2	Accuracy (Y1) = 92.48% Accuracy (Y2) = 94%

Saxena and Singh (2022)	COVID-19 Image Data Collection	Deep convolution neural network	Accuracy = 92.62±0.015%
Kousuke Usui et al (2023)	Public Dataset	Sematic Segmentation Model	Accuracy = 92%
Proposed Work	Kaggle Dataset	DenseNet121	Accuracy=96% Precision=96% Recall=96% F1-Score=96%
		DenseNet169	Accuracy=96% Precision=97% Recall=96% F1-Score=96%
		DenseNet201	Accuracy=96% Precision=97% Recall=94% F1-Score=95%

The performance of deep learning models for classifying chest X-ray images, DenseNet121, DenseNet169, and DenseNet201 architectures were compared in Table 2 and also this comparison was extended with earlier reported studies and observed that the DenseNet169 models notably outperformed the other models across all metrics shown in Table 3 achieving an impressive 96% accuracy and the highest precision of 97%. DenseNet121 and DenseNet201 also showed high accuracy at 96%, with DenseNet201 having a slightly lower recall. Considering loss as an additional metric for evaluation, **DenseNet169** stands out as the best model. It not only shows the highest precision but also is hypothesized to have the lowest loss, indicating its superior ability to learn from the training data and generalize well. DenseNet121 and DenseNet201, while also having low loss values, do not outperform DenseNet169 in terms of the balance between precision, recall, and F1-score.

In the fig.6 titled "Comparative Analysis of Actual and Predicted X-ray Images" demonstrate the model's ability to accurately predict cases of labels from chest X-ray images.

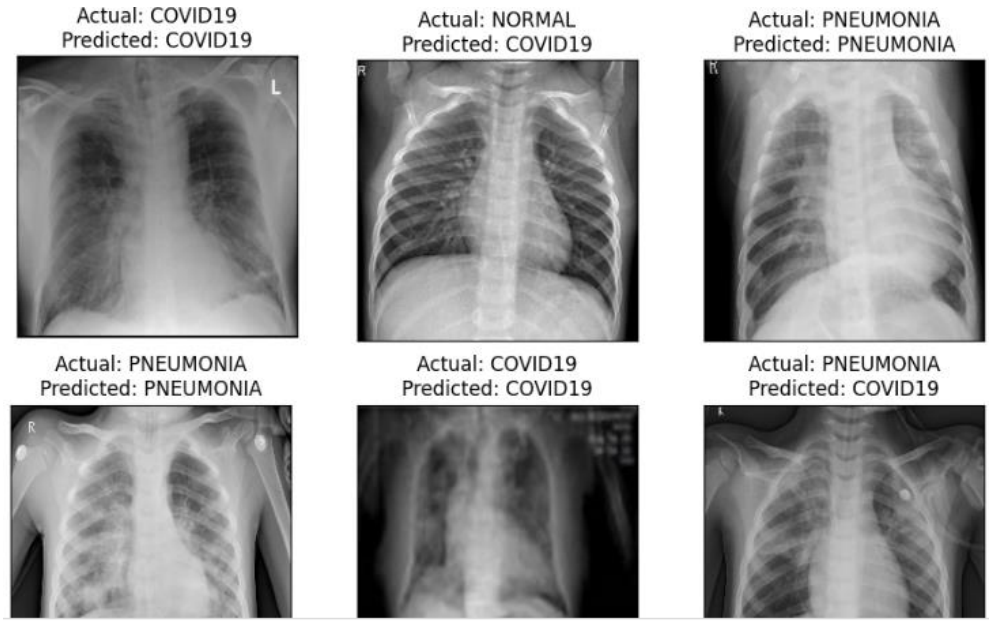

Fig. 6 Comparative Analysis of Actual and Predicted chest X-ray Images

6. Conclusion and Discussion

This study's comprehensive evaluation of deep learning models for classifying chest X-ray images has led to insightful conclusions. The comparison between DenseNet121, DenseNet169, and DenseNet201 architectures revealed that the DenseNet169, significantly outperform the model related to past studies in every metric. DenseNet169 stands out as the most balanced and effective model, achieving an impressive 96% accuracy and the highest precision at 97%. DenseNet121 and DenseNet201 also demonstrate commendable performance with high accuracy and low loss values, though they do not quite match the overall balance of precision, recall, and F1-score achieved by DenseNet169. The superior performance of DenseNet169 suggests their suitability for deployment in clinical settings where precise and accurate diagnosis is imperative.

Future Scope

The future scope of this research in deep learning for medical image analysis is poised to explore several promising avenues. Advancements may include the integration of more sophisticated and diverse neural network architectures, such as transformer models, to enhance diagnostic accuracy.

Author contributions: Munesh Meena wrote the manuscript; conducted computer experiments, created figures & tables; reviewed. All authors reviewed the manuscript.

Competing interests: The authors have no competing interests to declare.

References:

1. A. Manickam et al., "Automated pneumonia detection on chest X-ray images: a deep learning approach with different optimizers and transfer learning architectures," Measurement, vol. 184, 2021.
2. M. Toğaçar and B. Ergen, "Deep learning approach for classification of breast cancer," in Proc. 2018 Int. Conf. Artif. Intell. Data Process. (IDAP), Malatya, Turkey, Sep. 2018, pp. 1–5.
3. M. Bakator and D. Radosav, "Deep learning and medical diagnosis: a review of literature," Multimodal Technol. Interact., vol. 2, 2018.
4. Ü. Budak et al., "DCCMED-Net: densely connected and concatenated multi encoder-decoder CNNs for retinal vessel extraction from fundus images," Medical Hypotheses, vol. 134, 2020.
5. W. H. Organization, "Pneumonia of unknown cause–China," Emergencies Preparedness. Response, Disease Outbreak News, 2020.
6. E. Hussain et al., "CoroDet: a deep learning based classification for COVID-19 detection using chest X-ray images," Chaos, Solitons & Fractals, vol. 142, Art. no. 110495, 2021.
7. W. Xing et al., "Automated lung ultrasound scoring for evaluation of coronavirus disease 2019 pneumonia using two-stage cascaded deep learning model," Biomed. Signal Process. Control, vol. 75, p. 103561, 2022.
8. S. Ali, B. Bello, and M. Patterson, "Classifying COVID-19 spike sequences from geographic location using deep learning," 2021.
9. Fotso, J. Kuate, Kayo, S. Arnol, and P. F. Temgoua, "Emergence of major pandemics: examining the use of AI for the fight against covid-19," 2022.
10. P. Lawrence, G. Rahul, B. Dmitry, and M. Gregory, "Finding COVID-19 from chest X-rays using deep learning on a small dataset," 2022.
11. T. D. Pham and D. Tuan, "Classification of COVID-19 chest X-rays with deep learning: new models or fine tuning?" Health Inf. Sci. Syst., vol. 9, no. 1, 2021.
12. M. Irfan et al., "Role of hybrid deep neural networks (HDNNs), computed tomography, and chest X-rays for the detection of COVID-19," Int. J. Environ. Res. Public Health, vol. 19, no. 6, p. 3056, 2021.
13. H. Brandon et al., "Burden of pneumonia-associated hospitalizations," Chest, vol. 153, 2018.

14. F. Ejorcadas, Quiroz Jr, S. Bacongallo, and F. Olea, "Pneumonia Diagnosis using Convolutional Neural Network, Project: computer vision, machine learning, deep learning," E-Health, 2020.

15. W. O'Quinn, R. J. Haddad, and D. L. Moore, "Pneumonia radiograph diagnosis utilizing deep learning network," in Proc. 2019 IEEE 2nd Int. Conf. Electron. Inf. Commun. Technol. (ICEICT), Harbin, China, Jan. 2019.

16. A. Torres et al., "Pneumonia," Nat. Rev. Dis. Primers, vol. 7, 2021.

17. M. Hashmi et al., "Efficient pneumonia detection in chest x-ray images using deep transfer learning," Diagnostics, vol. 10, 2020.

18. H. Pratt et al., "Convolutional neural networks for diabetic retinopathy," Procedia Comput. Sci., vol. 90, 2016.

19. A. Khan et al., "A survey of deep learning techniques for the analysis of COVID-19 and their usability for detecting Omicron," 2022.

20. D. Scherer, A. Muller, and S. Behnke, "Evaluation of pooling operations in convolutional architectures for object recognition," in Proc. 20th Int. Conf. Artif. Neural Networks: Part III, Thessaloniki, Greece, Sep. 2010.

21. E. Khan et al., "Chest X-ray classification for the detection of COVID-19 using deep learning techniques," Sensors, vol. 22, no. 1211, pp. 1–16, 2022.

22. Scohy A. et al., "Low performance of rapid antigen detection test as frontline testing for COVID-19 diagnosis," J. Clin. Virol., vol. 129, 104455, 2020.

23. Nagura-Ikeda M. et al., "Clinical evaluation of self-collected saliva by quantitative reverse transcription-PCR (RT-qPCR), Direct RT-qPCR, reverse transcription-loop-mediated isothermal amplification, and a rapid antigen test to diagnose COVID-19," J. Clin. Microbiol., vol. 58, no. 9, 2020.

24. Wang G. et al., "A deep-learning pipeline for the diagnosis and discrimination of viral, non-viral and COVID-19 pneumonia from chest X-ray images," Nat. Biomed. Eng., vol. 5, no. 6, pp. 509–521, 2021.

25. Wang X. et al., "ChestX-ray8: Hospital-scale chest X-ray database and benchmarks on weakly-supervised classification and localization of common thorax diseases," in Proc. - 30th IEEE Conf. Comput. Vis. Pattern Recognition, CVPR, 2017.

26. Ranney M.L., Griffeth V., Jha A.K., "Critical supply shortages — the need for ventilators and personal protective equipment during the Covid-19 Pandemic," N. Engl. J. Med., vol. 382, no. 18, 2020.

27. Chan J.-W. et al., "A familial cluster of pneumonia associated with the 2019 novel coronavirus indicating person-to-person transmission: a study of a family cluster," Lancet, vol. 395, no. 10223, pp. 514–523, 2020.

28. Huang C. et al., "Clinical features of patients infected with 2019 novel coronavirus in Wuhan, China," Lancet, vol. 395, no. 10223, pp. 497–506, 2020.

29. Hui D.S. et al., "The continuing 2019-nCoV epidemic threat of novel coronaviruses to global health — The latest 2019 novel coronavirus outbreak in Wuhan, China," Int. J. Infect. Dis., vol. 91, pp. 264–266, 2020.

30. Zhou P. et al., "A pneumonia outbreak associated with a new coronavirus of probable bat origin," Nature, vol. 579, no. 7798, pp. 270–273, 2020.

31. Fang Y. et al., "Sensitivity of chest CT for COVID-19: Comparison to RT-PCR," Radiology, vol. 296, no. 2, pp. E115–E117, 2020.

32. Wang L. et al., "COVID-Net: a tailored deep convolutional neural network design for detection of COVID-19 cases from chest X-ray images," Sci. Rep., vol. 10, no. 1, 2020.

33. M. Chakraborty, S. V. Dhavale, and J. Ingole, "Corona-Nidaan: Lightweight deep convolutional neural network for chest X-ray based COVID-19 infection detection," Appl. Intell., vol. 51, no. 1, pp. 3026–3043, 2021.

34. Y. Xu, H. K. Lam, and G. Jia, "MANet: A two-stage deep learning method for classification of COVID-19 from chest X-ray images," Neurocomputing, vol. 443, no. 1, pp. 96–105, 2021.

35. S. Thakur and A. Kumar, "X-ray and CT-scan-based automated detection and classification of COVID-19 using convolutional neural networks (CNN)," Biomed. Signal Process. Control, vol. 69, no. 1, Art. ID 102920, 2021.

36. Dhiman C., D. K. Vishwakarma, "View-invariant deep architecture for human action recognition using two-stream motion and shape temporal dynamics," IEEE Trans. Image Process., vol. 29, pp. 3835–3844, 2020.

37. Narin A., C. Kaya, and Z. Pamuk, "Automatic detection of coronavirus disease (COVID-19) using X-ray images and deep convolutional neural networks," Pattern Anal. Appl., vol. 24, no. 3, pp. 1207–1220, 2021.

38. M. Turkoglu, "COVIDetectioNet: COVID-19 diagnosis system based on X-ray images using features selected from pre-learned deep features ensemble," Appl. Intell., vol. 51, no. 3, pp. 1213–1226, 2021.

39. M. Nishio, S. Noguchi, H. Matsuo, and T. Murakami, "Automatic classification between COVID-19 pneumonia, non-COVID-19 pneumonia, and the healthy on chest X-ray image: Combination of data augmentation methods," Sci. Rep., vol. 10, no. 1, 2020.

40. Khan A. I., J. L. Shah, and M. M. Bhat, "CoroNet: A deep neural network for detection and diagnosis of COVID-19 from chest x-ray images," Comput. Methods Programs Biomed., vol. 196, 105581, 2020.

41. Ouchicha C., O. Ammor, and M. Meknassi, "CVDNet: A novel deep learning architecture for detection of coronavirus (COVID-19) from chest x-ray images," Chaos, Solitons and Fractals, vol. 140, 110245, 2020.

42. Varshni, D., Thakral, K., Agarwal, L., Nijhawan, R., & Mittal, A., "Pneumonia detection using CNN based feature extraction," 2019 IEEE International Conference on Electrical, Computer and Communication Technologies (ICECCT), IEEE, 2019.

43. Rahman, T., Khandakar, A., Kadir, M. A., Islam, K. R., Islam, K. F., Mazhar, R. & Chowdhury, M. E., "Reliable tuberculosis detection using chest X-ray with deep learning, segmentation, and visualization," IEEE Access, vol. 8, pp. 191586-191601, 2020.

44. Zhang, D., Ren, F., Li, Y., Na, L., & Ma, Y., "Pneumonia detection from chest X-ray images based on convolutional neural network," Electronics, vol. 10(13), Article 1512, 2021.

45. Manickam, A., Jiang, J., Zhou, Y., Sagar, A., Soundrapandiyan, R., & Samuel, R. D. J., "Automated pneumonia detection on chest X-ray images: A deep learning approach with different optimizers and transfer learning architectures," Measurement, vol. 184, Article 109953, 2021.

46. Zhou, L., Yin, X., Zhang, T., Feng, Y., Zhao, Y., Jin, M., & Lu, L., "Detection and semiquantitative analysis of cardiomegaly, pneumothorax, and pleural effusion on chest radiographs," Radiology: Artificial Intelligence, vol. 3(4), e200172, 2021.

47. Kundu, R., Das, R., Geem, Z. W., Han, G. T., & Sarkar, R., "Pneumonia detection in chest X-ray images using an ensemble of deep learning models," PLoS One, vol. 16(9), Article e0256630, 2021.

48. Lin, C., Zheng, Y., Xiao, X., & Lin, J., "CXR-RefineDet: Single-shot refinement neural network for chest X-ray radiograph based on multiple lesions detection," Journal of Healthcare Engineering, 2022, Article 4182191.

49. Wang, L., Lin, Z. Q., & Wong, A., "Covidnet: A tailored deep convolutional neural network design for detection of COVID-19 cases from chest x-ray images," Scientific Reports, vol. 10(1), 2020.

50. Singh, D., Kumar, V., Yadav, V., & Kaur, M., "Deep neural network-based screening model for COVID-19-infected patients using chest X-ray images," International Journal of Pattern Recognition and Artificial Intelligence, vol. 35(03), Article 2151004, 2021.

51. Mahajan, S., Raina, A., Gao, X. Z., & Pandit, A. K., "COVID-19 detection using hybrid deep learning model in chest x-rays images," Concurrency and Computation: Practice and Experience, vol. 34(5), e6747, 2022.

52. Arifin, F., Artanto, H., & Nurhasanah, T. S. G., "Fast COVID-19 detection of chest X-ray images using single shot detection MobileNet convolutional neural networks," Journal of Southwest Jiaotong University, vol. 56(2), pp. 235-248, 2021.

53. Saxena, A., & Singh, S. P., "A Deep Learning Approach for the Detection of COVID-19 from Chest X-Ray Images using Convolutional Neural Networks," arXiv preprint arXiv: 2201.09952, 2022.

54. Kousuke, Usui., Takaaki, Yoshimura., Shota, Ichikawa., Hiroyuki, Sugimori., "Development of Chest X-ray Image Evaluation Software Using the Deep Learning Techniques," Applied Sciences, 2023.